AIAA JOURNAL
Vol. 35, No. 8, August 1997

Analysis of Streamline Curvature Effects on Wall-Bounded Turbulent Flows

Jiang Luo* and Budugur Lakshminarayana†
Pennsylvania State University, University Park, Pennsylvania 16802

This work deals with numerical analysis for the effects of surface curvature, particularly the concave curvature, on turbulent duct flows and boundary layers. A compressible Navier–Stokes code incorporating Reynolds stress models has been developed using a four-stage Runge–Kutta scheme. Numerical computations have been carried out for curved flows in 180-deg and 90-deg turning ducts and a turbulent boundary layer using Reynolds stress models with/without modifications to the dissipation rate (ε) equation. Various modifications to the ε equation are discussed. A quantitative relationship has been established between two seemingly different modifications to the ε equation. It is observed that the modeling of concave curvature effect is qualitatively different from the modeling of convex curvature effect. Detailed comparisons between computations and data indicate that, to capture the strong amplification of turbulence near a concave wall, the standard ε equation needs to be modified.

Nomenclature

C_f	= skin-friction coefficient, $\tau_w/(0.5\rho U_e^2)$
$C_{\varepsilon 1}, C_{\varepsilon 2}, C_\mu, C_c$	= constants in Eq. (2): 1.44, 1.92, 0.09, 0.2
$C^s_{\varepsilon 1}, C^s_{\varepsilon 2}$	= constants in Eq. (4): 0.43, 1.90
H	= duct height
k	= turbulent kinetic energy, $0.5\langle u_i u_i \rangle$
n	= coordinate normal to the surface
P	= static pressure
P_k	= production rate of k, $\langle -u_i u_j \rangle \partial U_i/\partial x_j$
R	= radius of curvature of reference streamline
Re, Re_θ	= Reynolds number ($U_m H/\nu$, $U_m\theta/\nu$)
Ri_t	= Richardson number, $(k/\varepsilon)^2(U/r^2)\partial(Ur)/\partial n$
r	= local radius of curvature of streamline
S	= invariant of strain rate, $\sqrt{2S_{ij}S_{ij}}$
S_{ij}	= strain rate, $(\partial U_i/\partial x_j + \partial U_j/\partial x_i)/2$
s	= streamwise coordinate along surface
U	= streamwise mean velocity
U_e	= freestream velocity at inlet
U_m	= bulk velocity
u, v, w	= fluctuating velocities in streamwise, normal (radial), and cross-stream directions (u, v, w representing rms values in Figs. 2–8)
$\langle u_i u_j \rangle$	= Reynolds stress
y	= coordinate normal to test wall
y^+	= wall distance variable, yu_τ/ν
δ	= boundary-layer thickness
ε	= dissipation rate of turbulent kinetic energy
θ	= angle into bend measured from bend entrance/momentum thickness
ν, ν_t	= laminar and turbulent kinematic viscosity, $C_\mu k^2/\varepsilon$
τ_w	= wall shear stress

Introduction

LONGITUDINAL surface curvature exerts a significant influence on turbulent boundary layers over curved bodies and flows through curved ducts. The skin-friction coefficient (and heat transfer rate), compared with that of a boundary layer on a flat surface, is decreased on a convex surface due to the damping of turbulence by the convex curvature, but it is increased on a concave surface due to the amplification of turbulence by the curvature (Refs. 1–3, etc.). Previous computational efforts, e.g., Refs. 1, 4, and 5, have demonstrated that the effects of curvature on turbulence intensity and structure must be predicted accurately to capture the boundary-layer development over curved surfaces. To predict the stabilizing and destabilizing curvature effects, it is necessary to make empirical modifications to eddy viscosity models.[1] Gibson et al.,[6] So et al.,[7] and Shima,[8] among others, have shown that the Reynolds stress model (RSM) can account for the curvature effects without empirical modifications. However, Park and Chung[9] modified the RSM with an additional curvature time scale to capture the curvature effects accurately.

The authors recently analyzed the turbulent flows in highly curved ducts with a RSM and observed that the RSM can successfully capture the large damping of turbulence near the convex wall but underpredicts the enhancement of turbulence near the concave wall.[10] The modeling of concave curvature effect appears to be quite different from the modeling of convex curvature effect. This may be attributed to the qualitatively different characters of these two effects, namely, the mere attenuation of preexisting eddies by convex curvature but reorganization of eddy structures by concave curvature, as suggested by Gillis and Johnston,[11] Muck et al.,[12] and Hoffman et al.,[13] etc.

As argued by many authors, a concave curved flow may become three dimensional due to the possible existence of Taylor–Gortler vortices. However, these longitudinal vortices have not been observed in some experiments. Barlow and Johnston[3] found that large scales in concave boundary layers exhibit a range of behavior from Taylor–Gortler vortices, when upstream nonuniformities are large, to energetic large eddies (radial inflows and outflows), when the upstream flow is uniform. They have observed that the enhancement of turbulence is mainly due to the large-scale eddies rather than the Taylor–Gortler vortices. These longitudinal vortices are found to cause only minor increases in the spanwise-averaged skin-friction coefficient. Hoffman et al.[13] also showed that the secondary effect of the vortices is less important than the primary effect of the concave surface curvature for moderately curved flows.

Barlow and Johnston[3] suggested that, for many applications, two-dimensional models should be adequate, provided that they can account for the slow development of the energetic large-scale eddies in concave boundary layers. The failure of the RSM (with the standard ε equation) in modeling these large eddies hence appears to be the major reason for the underprediction of turbulence enhancement by Luo and Lakshminarayana.[10] The major objective of the present paper is to improve the prediction of the concave curvature effects. Three strongly curved duct flows with/without streamwise pressure gradient will be analyzed using the RSM model. The modeling of

Received Sept. 14, 1996; revision received May 1, 1997; accepted for publication May 5, 1997.

*Ph.D. Candidate, Department of Aerospace Engineering; currently Senior Engineer, Solar Turbines, Inc., San Diego, CA 92101. Member AIAA.

†Evan Pugh Professor of Aerospace Engineering, and Director, Center for Gas Turbines and Power. Fellow AIAA.

the ε equation, including recent modifications to it, will be discussed and assessed.

Turbulence Models and Numerical Procedure

The Reynolds stress model employed in the present study is the RSM model of Gibson and Launder[14] with the exception of the diffusion term. The turbulent diffusion term is modeled with a simple isotropic stress diffusion model following the suggestion of Lien and Leschziner.[15] The standard ε equation can be written as

$$\frac{\mathrm{D}\varepsilon}{\mathrm{D}t} = \mathrm{Diff}(\varepsilon) + \frac{\varepsilon}{k}(C_{\varepsilon 1} P_k - C_{\varepsilon 2}\varepsilon) \tag{1}$$

where $\mathrm{D}\varepsilon/\mathrm{D}t$ stands for the convection of ε and $\mathrm{Diff}(\varepsilon)$ for the turbulent diffusion of ε. The preceding equation for ε is modeled in analogy to the equation for turbulent kinetic energy k.

As discussed in detail by Launder et al.[16] and Lumley,[17] it may be assumed that the local transfer rate of turbulent energy from the large-scale eddies to finer scale motions is essentially equal to the energy dissipation rate itself for steady flow close to local equilibrium, i.e., $P_k \approx \varepsilon$. Hence, for flows that are in local equilibrium, the source term in the ε equation might be modeled in terms of the turbulence production. This essentially implies that the production of dissipation is linearly proportional to the production of turbulent energy, whereas the destruction of dissipation is linearly proportional to the destruction of turbulent energy.

Modifications to Standard ε Equation

The modeled equation for ε, Eq. (1), has been used for over two decades and has been successful in predicting a variety of thin shear flows. Its weaknesses, such as the overprediction of the spread rate of the axisymmetric jet, have been recognized before, and a number of ad hoc modifications have been proposed. For example, to account for the streamline curvature effects, Launder et al.[4] (denoted as LPS) modified the destruction term in Eq. (1) to be $-C_{\varepsilon 2}(\varepsilon^2/k)(1 - C_c Ri_t)$, where $Ri_t = (k/\varepsilon)^2(U/r^2)\partial(Ur)/\partial n$ in curvilinear orthogonal (s, n) coordinate. Hanjalic and Launder (HL model[5]) modified the generation term in Eq. (1) to be $C_{\varepsilon 1}(\varepsilon/k)\nu_t(\partial U/\partial n)^2$. These two models seem to be different. However, for mildly or moderately curved flows, a quantitative relationship between them might be derived as follows. The additional sink term in the LPS[4] model can be added to the generation term, and Eq. (1) can be written as

$$\begin{aligned}
\frac{\mathrm{D}\varepsilon}{\mathrm{D}t} &= \mathrm{Diff}(\varepsilon) + \left(\frac{\varepsilon}{k}\right)\left\{\left[C_{\varepsilon 1}\nu_t\left(\frac{\partial U}{\partial n} - \frac{U}{r}\right)^2 \right.\right. \\
&\quad \left.\left. + \left(\frac{C_{\varepsilon 2}C_c}{C_\mu}\right)\nu_t\frac{U}{r^2}\frac{\partial(Ur)}{\partial n}\right] - C_{\varepsilon 2}\varepsilon\right\} \\
&= \mathrm{Diff}(\varepsilon) + \left(\frac{\varepsilon}{k}\right)\left\{C_{\varepsilon 1}\nu_t\left(\frac{\partial U}{\partial n}\right)^2\left[(1 - A)^2 \right.\right. \\
&\quad \left.\left. + \left(\frac{C_{\varepsilon 2}C_c}{C_{\varepsilon 1}C_\mu}\right)A(1 + A)\right] - C_{\varepsilon 2}\varepsilon\right\} \\
&\approx \mathrm{Diff}(\varepsilon) + \left(\frac{\varepsilon}{k}\right)\left\{C_{\varepsilon 1}\nu_t\left(\frac{\partial U}{\partial n}\right)^2(1 + A) - C_{\varepsilon 2}\varepsilon\right\}
\end{aligned} \tag{2}$$

where A is defined as $(U/r)/(\partial U/\partial n)$, the ratio of the extra strain rate produced by curvature to the primary shear strain. The empirical values for coefficients $C_{\varepsilon 1}$, $C_{\varepsilon 2}$, C_c, and C_μ have been used and the second-order term is neglected because A is normally very small for mildly to moderately curved flows. On the other hand, the HL model is given by

$$\begin{aligned}
\frac{\mathrm{D}\varepsilon}{\mathrm{D}t} &= \mathrm{Diff}(\varepsilon) + \left(\frac{\varepsilon}{k}\right)\left\{C_{\varepsilon 1}\nu_t\left(\frac{\partial U}{\partial n}\right)^2 - C_{\varepsilon 2}\varepsilon\right\} \\
&= \mathrm{Diff}(\varepsilon) + \left(\frac{\varepsilon}{k}\right)\left\{C_{\varepsilon 1}\nu_t\left(\frac{\partial U}{\partial n}\right)^2(1 + 0 \times A) - C_{\varepsilon 2}\varepsilon\right\}
\end{aligned} \tag{3}$$

This is actually an LPS-type model if the coefficient C_c in the LPS model is set to be 0.13 instead of 0.2. Thus, for mildly to moderately curved flows, the HL model appears to differ from the LPS model only in terms of the magnitude of the coefficient. Indeed, Rodi and Scheuerer[5] found that the LPS model is successful for curved boundary-layer flows and observed that the LPS model consistently has a stronger modification effect than the HL model. This is also consistent with Richmond and Patel's[18] observation that the HL model is able to capture the trend of curvature effects but underpredicts the magnitude.

Lumley[17] developed a new ε equation based on the concept of spectral energy transfer for nonequilibrium flows. The source term in this equation is modeled with the invariant strain rate (S) rather than P_k, thus removing the rigid linkage between the generation terms of the ε and k equations. By modeling the dynamic equation of the mean-square vorticity fluctuation, Shih et al.[19] derived a transport equation for the dissipation rate ε, the production term of which is similar to that of the ε equation by Lumley.[17] Shih et al.'s model is given as

$$\frac{\mathrm{D}\varepsilon}{\mathrm{D}t} = \mathrm{Diff}(\varepsilon) + C^s_{\varepsilon 1} S\varepsilon - C^s_{\varepsilon 2}\frac{\varepsilon^2}{k + \sqrt{\nu\varepsilon}} \tag{4}$$

The invariant strain rate S is defined as $S = \sqrt{(2S_{ij}S_{ij})}$, which is different from Lumley's[17] model, where the value of S is obtained from a separate transport equation. This new production term for the ε equation in fact modifies the time scale that controls the rate at which turbulent energy enters the spectral pipeline, as discussed in detail by Lumley.[17]

Numerical Procedure

A Navier–Stokes procedure, incorporating the RSM model, the standard ε equation, the LPS ε modification, and the Shih et al. ε model, has been developed based on the code described in Kunz and Lakshminarayana.[20] The mean-flow equations are integrated in time by the explicit four-stage Runge–Kutta scheme. The convection and diffusion terms are discretized on a nonstaggered grid using second-order accurate central differencing. Fourth-order and second-order artificial dissipation terms (with coefficients around 0.02 and 0.25)[20] are included to damp high wave number errors and to improve the shock capturing, respectively. For the present low-speed flows, the second-order artificial smoothing actually is not used. Eigenvalue scaling and local velocity scaling [using $(U/U_m)^2$] of artificial dissipation terms are used to avoid contamination of the solution by artificial dissipation.[20]

The RSM equations are discretized in space and integrated in time in the same way as the mean-flow equations. Because the convection terms in the RSM equations are discretized with central differencing, artificial dissipation is needed to prevent odd-even decoupling. It is observed that the inclusion of fourth-order artificial dissipation has not resulted in convergent solutions. Hence, a small amount of second-order artificial dissipation is added to the RSM equations. The required value of artificial dissipation for a convergent solution is fairly small (with the coefficient around 0.02). Local velocity scaling is also used to reduce the smoothing in the equations to zero inside the boundary layer. The artificial dissipation coefficient in the normal direction is kept as a small fraction, e.g., $\frac{1}{10}$, of that in the streamwise direction, which further reduces the influence of smoothing on the convergent solution to a negligible level. Note that the current level of second-order smoothing is much lower than that brought by the first-order accurate upwind-differencing scheme.

The iteration of the RSM equation in the present time-marching procedure is found to be stable, without the implementation of elaborate stabilizing measures such as those required for pressure-based methods. The implementation of the RSM model near the wall, including the matching of the RSM model with the near-wall model, has followed the procedure described by Lien and Leschziner.[21] The near-wall region ($y^+ < 70$) is handled by a one-equation model, in which only the k equation is solved while the near-wall ε profile is prescribed with empirical functions.[10] Unlike the low-Reynolds-number RSM (such as that used by So et al.[7]), the current Reynolds stress model is valid only for the fully turbulent region and cannot be used in the near-wall region. In other words, the RSM is

Table 1 Conditions (at bend entrance) for test cases

Authors	Turning angle, deg	δ/R_{in}	δ/R_{out}	Re	Re_θ	Remarks
Sandborn and Shin[22]	180	1.0	0.3	2.1×10^5	1.2×10^4	Constant width
Kim and Patel[23]	90	0.05	0.04	2.2×10^5	3×10^3	Constant width
Johnson and Johnston[24]	90	N/A	0.055	3.9×10^4	1.3×10^3	Variable width $\partial P/\partial s \approx 0$ on outer wall

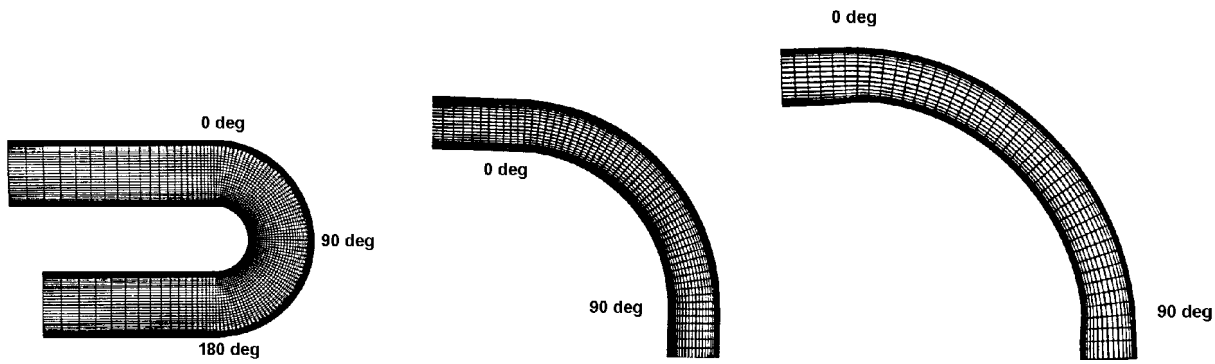

a) 180-deg duct[22] b) 90-deg duct[23] c) Concave boundary layer[24]

Fig. 1 Duct geometries and grids.

solved in the outer region ($y^+ > 70$), and boundary conditions for the Reynolds stress components ($\langle uu \rangle$, $\langle vv \rangle$, $\langle ww \rangle$, $\langle -uv \rangle$) are specified at $y^+ = 70$ grid line. Hence, the Reynolds stresses for $y^+ < 70$ are not computed in the current code. They are provided from the k equation, which is solved down to the wall. The typical distribution for $\langle uu \rangle$, $\langle vv \rangle$, $\langle ww \rangle$, and $\langle -uv \rangle$ in near-wall turbulence is employed, i.e., $\langle uu \rangle = 1.1k$, $\langle vv \rangle = 0.25k$, $\langle ww \rangle = 0.65k$, and $\langle -uv \rangle = 0.255k$.

Convergence criteria are taken as four decades drop of rms density residual and 2.5–3 decades drop of the rms residual for ε. The difference between the computed mass flow rates at the duct inlet and the exit is less than 0.2% of the inlet mass flow rate. The converged k–ε solution is used to initialize the computation with the RSM equations. It typically takes about 9000 steps to get a convergent RSM solution.

Results and Discussion

Description of Test Cases and Numerical Details

The cases computed in this paper include the two-dimensional flow in the 180-deg duct of Sandborn and Shin,[22] the midspan flow in the 90-deg rectangular duct of Kim and Patel,[23] and the turbulent boundary layer on the outer (concave) wall of the 90-deg duct measured by Johnson and Johnston.[24] The details of these test cases are given in Table 1.

The current Navier–Stokes code with the RSM model and the standard k–ε model has been validated against benchmark-quality data for flat-plate boundary-layer flows.[25] The computations of the preceding cases with different Reynolds numbers were carried out with an average inlet Mach number of approximately 0.2, to accommodate the compressible formulation of the current code. The inlet total pressure was adjusted to keep the Reynolds number the same as that in the measurement.

The geometries and grids of the ducts are shown in Fig. 1, where the bend region is plotted. The 251×141 (streamwise $\times$ normal) and 241×141 grids were generated by an algebraic method for the 180-deg duct and the two 90-deg ducts, respectively. A systematic grid independence study has been performed. For Kim and Patel's 90-deg duct flow, further refinement of the mesh (such as 281×141 and 281×161) has resulted in negligible difference in the solution. For instance, the relative difference in the computed skin-friction coefficients (C_f) at the bend exit, i.e., 90-deg location, is less than 0.5%. The first grid point near the wall is located around $y^+ = 1$. The inlet profiles for streamwise velocity, four individual Reynolds stress, and dissipation rate are obtained by computation of the developing flow in a long straight channel with the corresponding Reynolds number.[10]

180-deg Duct Flow

The predictions at two locations inside the bend ($\theta = 30$ and 90 deg) for Sandborn and Shin's[22] 180-deg duct flow ($Re = 2.1 \times 10^5$) are presented in this section. The predictions by the standard k–ε model are also included to highlight the performance of the three RSM models, namely, the RSM model with the standard ε equation, the LPS ε modification,[4] and the Shih et al.[19] ε model, respectively.

The predicted profiles of $\langle -uv \rangle$, $\langle uu \rangle$, $\langle vv \rangle$, and U at $\theta = 30$ deg are shown in Figs. 2a–2d, respectively. Near the inner wall, the turbulence has been greatly damped by convex curvature as well as by large flow acceleration, and the measured turbulent shear stress is close to zero over a large region (Fig. 2a). On the other hand, a large amplification of turbulence is observed near the concave wall. The k–ε model fails to account for the curvature effects and predicts a near-symmetric profile of $\langle -uv \rangle$, which is much higher than the data near the convex wall but lower than the data near the concave wall. The RSM with the standard ε model captures the turbulence damping very well but underpredicts the amplification of turbulence as stated earlier. The two modified ε models are seen to provide significant improvement in capturing the concave curvature effects over the standard ε model (Figs. 2a–2c).

As seen in Figs. 2b and 2c, the predicted streamwise fluctuation velocity ($u = \sqrt{\langle uu \rangle}$) by all the RSM models is larger than the normal fluctuation velocity ($v = \sqrt{\langle vv \rangle}$) near the concave wall, in agreement with the data. The isotropic k–ε model predicts close values for all the three normal stresses, among which $\langle uu \rangle$ is underpredicted near the concave wall, whereas $\langle vv \rangle$ is overpredicted near the convex wall. The mean velocity profiles (Fig. 2d) predicted by all the models are in good agreement with the data because the mean flow at this location is dominated by large pressure gradients and is not sensitive to the predicted levels of turbulence.

The major features of the flow at $\theta = 90$ deg (Fig. 3) are similar to those observed at $\theta = 30$ deg. All the RSM models capture the complete damping of turbulence near the convex wall very well. Both the predicted and measured mean velocity profiles show very thin boundary layers near the convex wall (Fig. 3d). Near the concave wall, strong turbulent mixing brings high-momentum fluid towards the wall, creating full velocity profile. The RSM with LPS ε model and the Shih et al. ε model predict the highest level of turbulence amplification (Figs. 3a–3c) and hence the fullest velocity profile near the concave wall, being in the closest agreement with the data. The RSM with the standard ε model is seen to capture the trend of the effect of concave curvature on turbulence but underpredicts the magnitude.

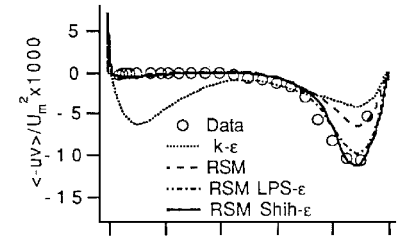

a) Turbulent shear stress

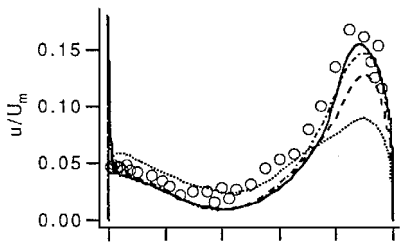

b) Streamwise rms turbulent velocity

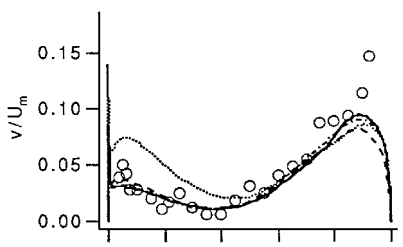

c) Radial rms turbulent velocity

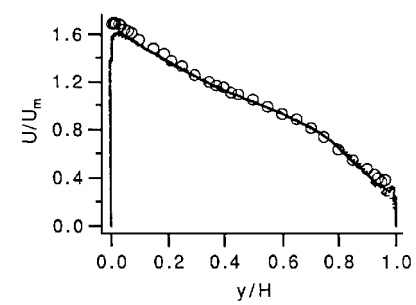

d) Streamwise mean velocity

Fig. 2 Profiles of 180-deg duct flow at $\theta = 30$ deg (Ref. 22).

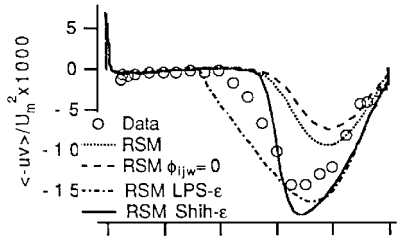

a) Turbulent shear stress

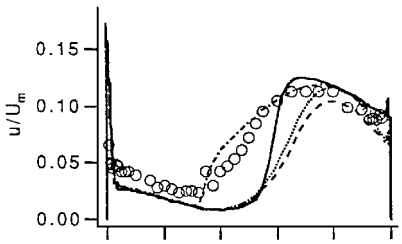

b) Streamwise rms turbulent velocity

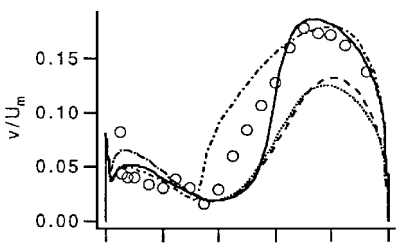

c) Radial rms turbulent velocity

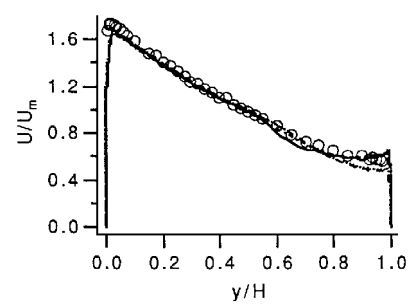

d) Streamwise mean velocity

Fig. 3 Profiles of 180-deg duct flow at $\theta = 90$ deg (Ref. 22).

Many authors have observed a very large increase in the radial component of Reynolds stress ($\langle vv \rangle$) in concave boundary layers, which can also be seen in Fig. 3c. Unlike the location $\theta = 30$ deg, the radial fluctuation velocity v at $\theta = 90$ deg is now as large as 1.5 times the streamwise fluctuation velocity u. This feature is quite unusual for attached turbulent shear flows. The high value of radial fluctuation velocity is caused by the large-scale radial inflows and outflows, which are induced directly by the centrifugal instability.

The RSM with the standard ε model is seen to underpredict the values for both u and v (Figs. 3b and 3c). The underprediction of v seems to be more serious than that of u. This may be attributed to the near-wall model for pressure–strain correlation (ϕ_{ijw}) in Gibson and Launder's[14] model, which is known to have excessive damping effect for normal Reynolds stress, i.e., $\langle vv \rangle$, even far away from the wall. However, a test run has been made using the RSM with ϕ_{ijw} set to zero near the concave wall and the standard ε model. As seen in Figs. 3b and 3c, this ad hoc model provides only slight improvement in predicting the value of $\langle vv \rangle$, while providing less satisfactory predictions for $\langle uv \rangle$ and $\langle uu \rangle$. This numerical experiment indicates that the underprediction of turbulence by the RSM with the standard ε model should not be attributed to the near-wall modeling for pressure–strain correlation. The underprediction is more likely to be caused by the problem with the standard ε model. Indeed, the two modified ε models are seen to capture the amplification of turbulence much better than the standard ε model (Figs. 3a–3c).

It is somewhat surprising to see that the LPS ε model[4] and the Shih et al. ε model[19] provide similar predictions for turbulence amplification, although the development of these two models followed different arguments. The source term of the Lumley[17] and the Shih et al.[19] ε models differs from that of the standard ε model because the former modifies the time scale for spectral energy transfer.[17] By modifying the sink term, the LPS model essentially increases the time scale for spectral energy transfer in the concave region and reduces it in the convex region as seen in Eq. (2). Both modifications have removed the rigid linkage between the generation terms of ε and k equations. Note that, unlike the LPS ε model, the extension of the Lumley[17] and the Shih et al.[19] ε models to three-dimensional flows is straightforward.

Indeed, the failure of the standard ε model should be attributed mainly to the modeling of its generation term, which is based on the assumption that the production of dissipation should keep pace with the production of turbulent energy, i.e., without any lag in the process of spectral energy transfer. This assumption is known to be accurate only for the flows in local equilibrium. But the flow near the concave wall is not in local equilibrium.

If there is no lag in the transfer of energy from large eddies to small eddies, then the energy level at small eddies (hence the level of dissipation) in a concave boundary layer should be significantly higher than that in a flat boundary layer because it is well known that the energy level of large eddies in a concave boundary layer is

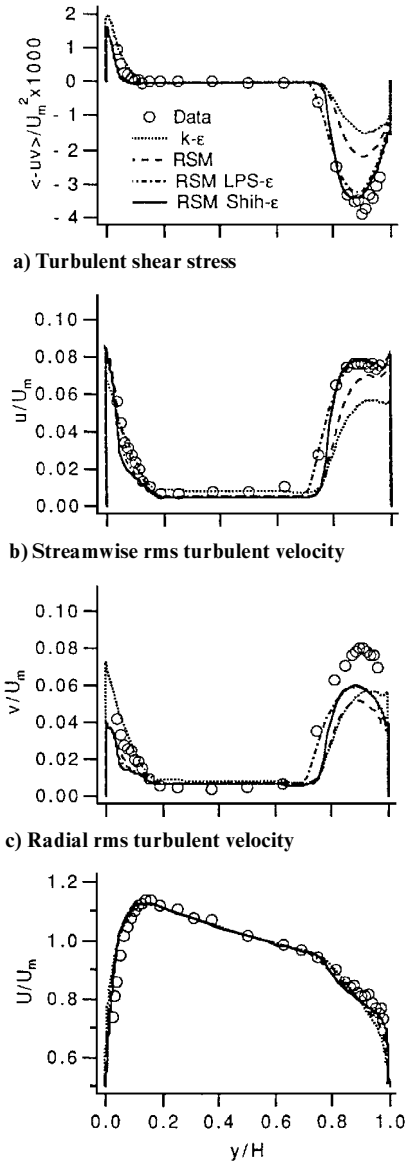

a) Turbulent shear stress

b) Streamwise rms turbulent velocity

c) Radial rms turbulent velocity

d) Streamwise mean velocity

Fig. 4 Profiles of 90-deg duct flow at $\theta = 45$ deg (Ref. 23).

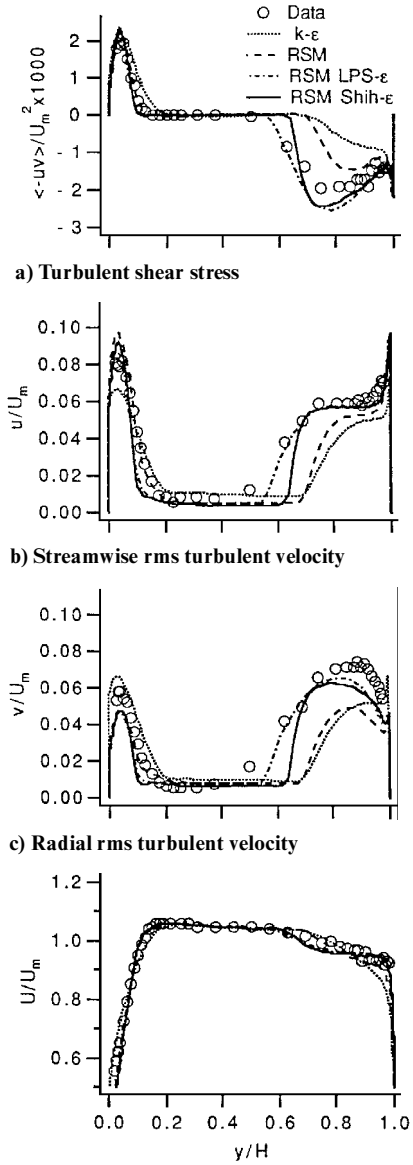

a) Turbulent shear stress

b) Streamwise rms turbulent velocity

c) Radial rms turbulent velocity

d) Streamwise mean velocity

Fig. 5 Profiles of 90-deg duct flow at 0.5*H* downstream of bend.[23]

much higher than that in a flat boundary layer. However, through the measurement of energy spectra, Barlow and Johnston[3] found that "at high frequencies, the energy content of the turbulence is about the same as in the flat boundary layer for all y-locations, suggesting that the small-scale turbulence structure is essentially unaffected by curvature." In their direct numerical simulation (DNS) of a mildly curved channel flow, Moser and Moin[26] concluded that "the dissipation terms, which are dominated by the small scales, are in good agreement on the two walls (convex and concave). . . . This suggests that curvature has a minimal effect on small scale of turbulence."

All of these observations indicate that there is a lag in the development of true dissipation in concave boundary layers as suggested by Lumley[17] for evolving nonequilibrium flows. Thus, to capture the large amplification of turbulence in concave boundary layers, the generation term in the ε equation should not keep pace with that in the k equation. This is the reason for the significant improvement obtained by both the LPS ε model and Lumley and Shih et al.'s ε model, as has been demonstrated in Fig. 3.

90-deg Duct Flow

The predicted profiles for $\langle -uv \rangle$, $\langle uu \rangle$, $\langle vv \rangle$, and U at $\theta = 45$ deg and $0.5H$ downstream of the bend for Kim and Patel's[23] flow are presented in Figs. 4 and 5, respectively. The curvature parameter (δ/R) of this flow is considerably smaller than that of Sandborn and Shin[22] (Table 1). The opposite effects of convex and concave curvatures are still quite significant as seen from the highly nonsymmetric profiles of turbulence quantities. The experimental uncertainty is reported to be 1.5% in streamwise mean velocity (U), 5% in $\langle uu \rangle$, and 10% in other turbulence stresses.[23] At both streamwise locations, the turbulence level near the concave wall is significantly underpredicted by the RSM with the standard ε model. The predictions by the RSM with both modified ε models are in significantly closer agreement with the data. This gives further support to the argument made earlier.

At $\theta = 45$ deg, the measurement has nearly equal values for the three Reynolds stress components. The RSMs with both modified ε models capture $\langle uu \rangle$ quite well but still underpredict the values of $\langle vv \rangle$ near the concave wall (Figs. 4a–4c). At $0.5H$ downstream of the bend, the measured radial fluctuation velocity v is even slightly higher than the streamwise velocity u near the concave wall (Figs. 5a–5c). The RSMs with both modified ε models capture the turbulence quantities near the concave wall much better than the RSM with the standard ε model.

The predicted skin-friction coefficient C_f on the convex wall of this duct is shown in Fig. 6a. The predicted values of C_f from all the RSM models are about the same and in good agreement with the data. The standard k–ε model, however, substantially overpredicts the value of C_f due to its overprediction of the turbulent shear stress as shown earlier. On the concave wall, as seen in Fig. 6b, the levels of C_f predicted by different models are seen to be proportional to the predicted levels of turbulent energy and $\langle -uv \rangle$. The standard k–ε

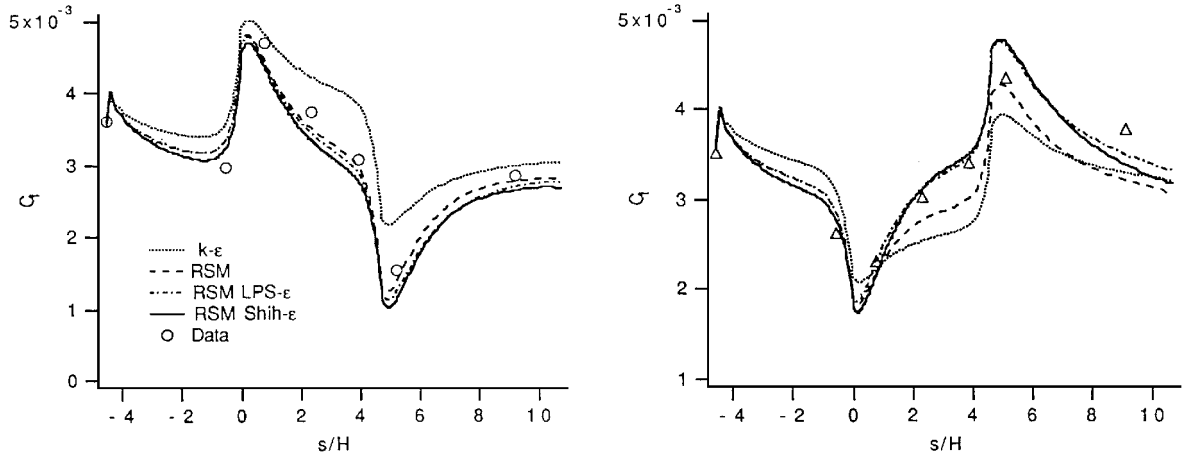

Fig. 6 Skin-friction coefficients for 90-deg duct flow.[23]

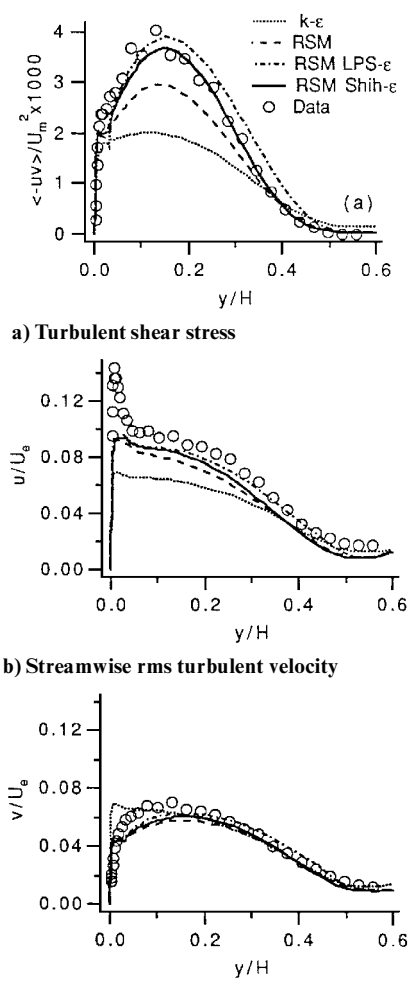

Fig. 7 Profiles of concave boundary-layer flow at $\theta = 30$ deg (Ref. 24).

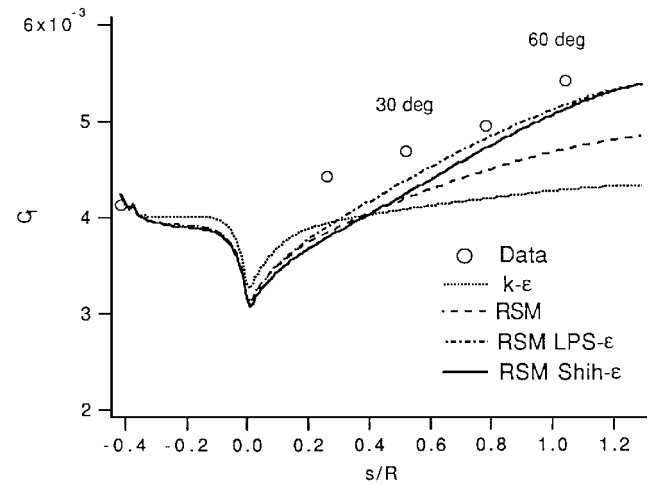

Fig. 8 Skin-friction coefficient for concave boundary layer.[24]

model underpredicts the value of C_f due to its underprediction of $\langle -uv \rangle$. The RSM with the standard ε model also underestimates the C_f because it has not captured the large amplification of turbulence near the concave wall. The RSMs with the two modified ε models predict the highest level of turbulence and hence the highest C_f, both being in best agreement with the data.

Concave Turbulent Boundary Layer

In both the geometries presented earlier, the boundary layers near the concave wall are subject to a fairly strong streamwise pressure gradient. To isolate the effects of concave curvature from those caused by the pressure gradient, the inner wall in Johnson and Johnston's[24] 90-deg duct was contoured to minimize the pressure gradient on the outer (test) wall. The turbulent velocity fluctuations and shear stress profiles are presented in Figs. 7a–7c for $\theta = 30$ deg where y starts from outer wall. The four models provide predictions in different levels of agreement with the data, similar to what has been observed for the aforementioned cases with the influence of pressure gradient. This further supports the argument that the standard ε model must be modified to capture the turbulence amplification in concave boundary layers with/without pressure gradients.

Finally, the predicted C_f is shown in Fig. 8. The behavior of C_f is different from that of Kim and Patel's[23] duct because the streamwise pressure gradient is now much lower. The predicted values of C_f by different turbulence models are seen to correspond to the predicted turbulence quantities. The RSMs with the modified ε models provide the best predictions for turbulence quantities and hence for the skin-friction coefficient.

Concluding Remarks

Numerical computations using Reynolds stress models have been carried out to investigate the effects of surface curvature, particularly concave curvature, on turbulent duct flows and boundary layers. The modeling of concave curvature effect is observed to be qualitatively different from the modeling of convex curvature effect. The RSM model is very successful in predicting the turbulence damping due to convex curvature but underpredicts the magnitude of turbulence amplification due to concave curvature. The present analyses indicate that there is a lag in the development of true dissipation in concave boundary layers. To capture the large amplification of turbulence in concave boundary layers, the generation term in the ε equation should not keep pace with that in the k equation. A

quantitative relationship has been derived between the modifications to the ε equation by Launder et al.[4] and Hanjalic and Launder.[5] Detailed comparisons between computations and data indicate that the Launder et al.[4] ε model and the newly developed ε model due to Lumley[17] and Shih et al.[19] provide substantially improved predictions for the concave curvature effects. The Lumley and Shih et al. ε model also has one significant advantage over the earlier model by Launder et al., namely, the extension of the former to three-dimensional flows is straightforward.

Acknowledgments

This work was supported by NASA through Contract NAS 8-38867 monitored by Lisa Griffin of the Marshall Space Flight Center (MSFC). We wish to acknowledge NASA for providing the Supercomputer resources at NASA Ames Research Center and MSFC. We would also like to thank V. A. Sandborn, V. C. Patel, W. J. Kim, and J. P. Johnston for providing the experimental data.

References

[1]Bradshaw, P., "Effects of Streamline Curvature on Turbulent Flow," AGARDograph 169, 1973.

[2]So, R. M. C., and Mellor, G., "Experiment on Convex Curvature Effects in Turbulent Boundary Layers," *Journal of Fluid Mechanics*, Vol. 60, 1973, p. 43.

[3]Barlow, R. S., and Johnston, J. P., "Structure of a Turbulent Boundary Layer on a Concave Surface," *Journal of Fluid Mechanics*, Vol. 191, 1988, p. 137.

[4]Launder, B., Priddin, C. H., and Sharma, B., "The Calculation of Turbulent Boundary Layers on Curved and Spinning Surfaces," *Journal of Fluids Engineering*, Vol. 98, March 1977, p. 753.

[5]Rodi, W., and Scheuerer, G., "Calculation of Curved Shear Layers with Two-Equation Turbulence Models," *Physics of Fluids*, Vol. 26, June 1983, p. 1422.

[6]Gibson, M. M., Jones, W. P., and Younis, B. A., "Calculation of Turbulent Boundary Layers on Curved Surfaces," *Physics of Fluids*, Vol. 24, March 1981, p. 386.

[7]So, R. M. C., Lai, Y. G., and Hwang, B. C., "Near-Wall Turbulence Closure for Curved Flows," *AIAA Journal*, Vol. 29, No. 8, 1991, pp. 1202–1213.

[8]Shima, N., "Prediction of Turbulent Boundary Layers with a Second-Moment Closure: Part II—Effects of Streamline Curvature and Spanwise Rotation," *Journal of Fluids Engineering*, Vol. 115, March 1993, pp. 64–69.

[9]Park, S. B., and Chung, M. K., "Reynolds Stress Model Analysis of Turbulent Flow over a Curved Axisymmetric Body," *AIAA Journal*, Vol. 29, No. 4, 1991, pp. 591–594.

[10]Luo, J., and Lakshminarayana, B., "Prediction of Strongly Curved Turbulent Duct Flows with Reynolds Stress Model," *AIAA Journal*, Vol. 35, No. 1, 1997, pp. 91–98.

[11]Gillis, J. C., and Johnston, J. P., "Turbulent Boundary Layer Flow and Structure on a Convex Wall and Its Redevelopment," *Journal of Fluid Mechanics*, Vol. 135, 1983, p. 123.

[12]Muck, K. C., Hoffmann, P. H., and Bradshaw, P., "The Effect of Convex Curvature on Turbulent Boundary Layers," *Journal of Fluid Mechanics*, Vol. 161, 1985, pp. 347–370.

[13]Hoffmann, P. H., Muck, K. C., and Bradshaw, P., "The Effect of Concave Surface Curvature on Turbulent Boundary Layers," *Journal of Fluid Mechanics*, Vol. 161, 1985, pp. 371–403.

[14]Gibson, M. M., and Launder, B., "Ground Effects on Pressure Fluctuations in the Atmospheric Boundary Layer," *Journal of Fluid Mechanics*, Vol. 86, 1978, p. 491.

[15]Lien, F. S., and Leschziner, M. A., "Assessment of Turbulence-Transport Models Including Non-Linear RNG Eddy-Viscosity Formulation and Second-Moment Closure for Flow over a Backward-Facing Step," *Computers and Fluids*, Vol. 23, No. 8, 1994, pp. 983–1004.

[16]Launder, B. E., Reynolds, W. C., and Rodi, W., *Turbulence Models and Their Applications*, Editions Eyrolles, Paris, France, 1984.

[17]Lumley, J. L., "Some Comments on Turbulence," *Physics of Fluids A*, Vol. 4, Feb. 1992, p. 203.

[18]Richmond, M. C., and Patel, V. C., "Convex and Concave Surface Curvature Effects in Wall-Bounded Turbulent Flows," *AIAA Journal*, Vol. 29, No. 6, 1991, p. 895.

[19]Shih, T.-H., Liou, W. W., Shabbir, A., Yang, Z., and Zhu, J., "A New k–ε Eddy-Viscosity Model for High Reynolds Number Turbulent Flows," *Computers and Fluids*, Vol. 24, No. 3, 1995, pp. 227–238.

[20]Kunz, R. F., and Lakshminarayana, B., "Three-Dimensional Navier–Stokes Computation of Turbomachinery Flows Using an Explicit Numerical Procedure and a Coupled k–ε Turbulence Model," *Journal of Turbomachinery*, Vol. 114, July 1992, p. 627.

[21]Lien, F. S., and Leschziner, M. A., "A General Non-Orthogonal Finite-Volume Algorithm for Turbulent Flow at All Speeds Incorporating Second-Moment Closure, Part 1: Numerical Implementation," *Computer Methods in Applied Mechanics and Engineering*, Vol. 114, 1994, p. 123.

[22]Sandborn, V. A., and Shin, J. C., "Water Flow Measurements in a 180 Degree Turn-Around Duct," Contract Rept. for Marshall Space Flight Center, Colorado State Univ., Fort Collins, CO, June 1989.

[23]Kim, W. J., and Patel, V. C., "An Experimental Study of Boundary-Layer Flow in a Curved Rectangular Duct," *ASME Fluids Engineering Conference*, FED-Vol. 146, American Society of Mechanical Engineers, New York, 1993, pp. 13–28.

[24]Johnson, P. L., and Johnston, J. P., "The Effects of Grid-Generated Turbulence on a Flat and Concave Turbulent Boundary Layers," Dept. of Mechanical Engineering, Stanford Univ., Rept. MD-53, Stanford, CA, 1989.

[25]Luo, J., "Navier–Stokes Computation and Turbulence Modeling for Turbine Viscous Flow & Heat Transfer," Ph.D. Thesis, Dept. of Aerospace Engineering, Pennsylvania State Univ., University Park, PA, Feb. 1996.

[26]Moser, R. D., and Moin, P., "The Effect of Curvature in Wall-Bounded Turbulent Flows," *Journal of Fluid Mechanics*, Vol. 175, 1987, p. 479.

P. R. Bandyopadhyay
Associate Editor